

## Viscous-fingering minimization in uniform three-dimensional porous media

Eduardo O. Dias\*

*Departamento de Física, Universidade Federal de Pernambuco, Recife, Pernambuco 50670-901, Brazil*  
(Received 30 September 2013; revised manuscript received 30 October 2013; published 10 December 2013)

In this paper, we consider a radial displacement of a viscous fluid by another one of much lower viscosity through a three-dimensional uniform porous medium. It is well known that when a less viscous fluid is pumped at a constant injection rate, very complex interfacial patterns are formed. The control and eventual suppression of these instabilities are relevant to a large number of areas in science and technology. Here, we use a variational approach to search for an analytical form of an optimal flow rate so that the interface between two almost neutrally buoyant fluids grows, but the emergence of interfacial disturbances is minimized. We find a closed analytical solution for the ideal flow rate which surprisingly does not depend on either the properties of the fluids or the permeability of the porous medium.

DOI: [10.1103/PhysRevE.88.063007](https://doi.org/10.1103/PhysRevE.88.063007)

PACS number(s): 47.56.+r, 47.20.Ma, 47.55.N-, 47.15.gp

### I. INTRODUCTION

Viscous-fingering instability, observed first by Saffman and Taylor [1], has been actively studied for over half a century [2]. This phenomenon occurs when a less viscous fluid displaces another fluid of higher viscosity in a porous medium or in a confined geometry of a Hele-Shaw cell. The fluid dynamics equations of these two systems are similar, and because the Hele-Shaw cell setup is much more accessible in the laboratory, it has offered numerous contributions to the better understanding of Saffman-Taylor instability. In particular, Hele-Shaw radial flow presents fingerlike structures whose tips tend to split, giving rise to complex interfacial morphologies. This fluid dynamic problem is an archetype for a wide range of fields, including research in oil recovery processes in porous media [3], fluid mixing [4], flow in granular media [5], microdischarges in plasmas [6], and biodynamics of cell fragmentation [7].

It is known that the emergence of a ramified fingering caused by viscous driven instability is a major factor in degrading oil recovery from underground petroleum reservoirs [3]. Therefore, it is of scientific and technological relevance to search for a way to control and inhibit the growth of bifurcated patterns. Regarding this point, controlling viscous fingering has generated considerable interest in recent years both in a Hele-Shaw setup and in porous media flow. Some recent control methods have been employed by utilizing the following distinct procedures: manipulating the injection rate [8–15], modifying the original structure of the parallel Hele-Shaw plates [16,17], and adding a wetting layer of surfactant which makes the surface tension depend on the interface curvature [18,19]. On the other hand, there are several works in porous media that try to enhance oil recovery [3,20–27]: one of the usual methods is performed by flooding the reservoir with a polymer before the water injection process.

In a macroscopically uniform porous medium, the onset of instability under immiscible displacement was first understood by the theory developed by Chuoke *et al.* [28], and by an extension made by Neuman and Chen [29]. Chuoke *et al.* have proposed that the front is subjected to a stabilizing force

proportional to macroscopic curvature of the interface, where the proportionality factor represents an effective surface tension. Furthermore, Ref. [28] observed that when a higher viscosity of the displaced fluid is considered or lower interfacial tension at the interface is assumed, relatively small fingers arise at the interface. This behavior is similar to one verified in Hele-Shaw flows. Viscous driven instability is also highly influenced by the wetting properties of the fluids. References [30,35] observed that in oil-wet media, the fingers form a fractal pattern with size on the order of the medium pores. On the other hand, in water-wet media the fingers are much wider in comparison with those in oil-wet media [36]. In addition, there are alternative theories for porous media flows that consider variations in the saturation behind the front which can reduce the mobility of the fluids [31], and others models that assume heterogeneity of the porous medium [32,33]. Nevertheless, the theory developed in Ref. [28] explains satisfactorily the experimental observations of Refs. [28,34,36,37].

In this work, we consider the Chuoke *et al.* theory for a three-dimensional uniform porous medium flow. Then we use a variational method, which was proposed recently in Ref. [8], in order to minimize the perturbations of a radially growing interface. This approach has been successfully verified for the driven injection flow in a radial Hele-Shaw cell. The main question of this variational protocol can be expressed as follows: if one wants to inject a certain volume of fluid in a given time, what would be the optimal time-dependent injection rate  $Q(t)$  so that the perturbation amplitudes could be minimized? We apply this method in a radial flow of an inviscid fluid displacing another viscous one completely in a uniform porous medium. This natural extension of the system used in Ref. [8] is of technological importance because of its greater similarity to the real oil recovery process.

### II. LINEAR STABILITY CALCULATION

#### A. Derivation of the linear growth rate

Consider a three-dimensional uniform porous medium containing an incompressible fluid of viscosity  $\eta_1$  initially with a spherical shape of radius  $R_0$ , and with its center located at the origin of the coordinate system. Another fluid with much higher viscosity  $\eta_2$  surrounds fluid 1 filling all porous

\*[eduardodias@df.ufpe.br](mailto:eduardodias@df.ufpe.br)

medium. Then, the less viscous fluid is injected at a rate  $Q(t)$  (volume covered per unit time, which may depend on time) at the origin of the coordinate system displacing the more viscous one completely. This procedure promotes an unstable growth of the interface, in which its thickness is assumed to be much thinner than the wavelengths of the perturbation. Linear stability analysis of the problem considers harmonic distortions of a nearly spherical fluid-fluid interface whose radius evolves according to

$$\mathcal{R}(\theta, \phi, t) = R(t) + \zeta(\theta, \phi, t), \quad (1)$$

where  $\theta$  is the polar angle,  $\phi$  is the azimuthal angle,  $\zeta(\theta, \phi, t)$  represents the surface perturbation in spherical coordinates, and  $R = R(t)$  is the time-dependent unperturbed radius of the fluid-fluid interface. For convenience, we write  $\zeta(\theta, \phi, t)$  in terms of spherical harmonics

$$\zeta(\theta, \phi, t) = \sum_{l=1}^{\infty} \sum_{m=-l}^l \zeta_{lm}(t) Y_{lm}(\theta, \phi), \quad (2)$$

with  $\zeta_{lm}(t)$  the harmonic spherical amplitudes. Finally, the volume conservation leads to the equation

$$R(t) = \left( R_0^3 + \frac{3}{4\pi} \int_0^t Q(t') dt' \right)^{1/3}. \quad (3)$$

The hydrodynamic equation in a uniform porous medium is governed by Darcy's law [28],

$$\mathbf{v}_i = -\frac{k}{\eta_i} (\nabla p_i - \rho_i g \hat{\mathbf{z}}), \quad (4)$$

where  $i = 1$  (2) for the displacing fluid (displaced fluid),  $\mathbf{v}_i = \mathbf{v}_i(r, \theta, \phi, t)$  is the three-dimensional velocity,  $k$  is the permeability which is a property of the medium,  $\eta_i$  is the fluid viscosity,  $p_i = p_i(r, \theta, \phi, t)$  is the fluid pressure,  $g$  is the gravitational acceleration, and  $\rho_i$  is the fluid density. From now on, we consider that both fluids have approximately the same density  $\rho_1 \approx \rho_2$ , and  $\eta_1 \ll \eta_2$ . For a homogeneous, isotropic porous medium,  $k$  is a constant in space within each region occupied by both fluids. On this basis, we can define a velocity potential  $\Phi_i$ , where  $\mathbf{v}_i = -\nabla \Phi_i$ . By noting that  $\rho_i g \hat{\mathbf{z}} = \nabla(\rho_i g z)$ , and subtracting  $\eta_i \Phi_i$  in Eq. (4) for  $i = 1$  and 2 evaluated at the fluid-fluid perturbed interface ( $r = \mathcal{R}$ ), we obtain

$$A \frac{(\Phi_1|_{\mathcal{R}} + \Phi_2|_{\mathcal{R}})}{2} - \frac{(\Phi_1|_{\mathcal{R}} - \Phi_2|_{\mathcal{R}})}{2} = -\frac{k[(p_1 - p_2) + (\rho_2 - \rho_1)gz]|_{\mathcal{R}}}{\eta_1 + \eta_2}, \quad (5)$$

where  $A = (\eta_2 - \eta_1)/(\eta_2 + \eta_1)$ . Since we consider  $\eta_1 \ll \eta_2$  ( $A = 1$ ) and  $|[(\rho_1 - \rho_2)gz]|_{\mathcal{R}} \ll |(p_1 - p_2)|_{\mathcal{R}}$ , we have

$$\Phi_2|_{\mathcal{R}} = -\frac{k}{\eta_2} (p_1 - p_2)|_{\mathcal{R}}. \quad (6)$$

For the injection-driven flow, we consider the incompressibility condition  $\nabla \cdot \mathbf{v}_i = \mathbf{0}$  so that the velocity potential satisfies  $\nabla^2 \Phi_i = \mathbf{0}$ . The solution for the displaced viscous fluid is given by [38]

$$\Phi_2(r, \theta, \phi) = \frac{Q(t)}{4\pi r} + \sum_{l=1}^{\infty} \sum_{m=-l}^l \Phi_{lm}(t) \left( \frac{r}{R} \right)^{-(l+1)} Y_{lm}(\theta, \phi). \quad (7)$$

To find a relation between  $\Phi_{lm}(t)$  in Eq. (7) and  $\zeta_{lm}(t)$ , we consider the kinematic boundary condition which states that the normal components of fluid velocity at the interface equal the velocity of the interface. Keeping terms up to first order in  $\zeta$ , the kinematic boundary condition reads  $\partial \mathcal{R} / \partial t = (-\partial \Phi_2 / \partial r)_{r=\mathcal{R}}$ . Using the orthonormality of the spherical harmonics and solving for  $\Phi_{lm}(t)$  consistently yields

$$\Phi_{lm}(t) = \frac{1}{(l+1)} \left[ R \dot{\zeta}_{lm} + \frac{Q(t)}{2\pi R^2} \zeta_{lm} \right], \quad (8)$$

where the overdot denotes total time derivative.

Another important boundary condition at the interface, which is analogous to the Young-Laplace equation, has been proposed by Chuoke *et al.* [28]. It relates the curvature to the pressure jump across the fluid-fluid interface by the expression

$$(p_1 - p_2)|_{\mathcal{R}} = \sigma^* \left[ \frac{1}{r_a} + \frac{1}{r_b} \right] + p_c(t), \quad (9)$$

where  $\sigma^*$  is an effective (macroscopic) surface tension coefficient,  $r_a$  and  $r_b$  are the two principal radii of curvature of the interface, and  $p_c(t)$  is related to capillary pressure drops across microscopic interfaces (depending solely on the time and not on the interface curvature). Chuoke *et al.* have assumed that  $\sigma^* = C\sigma$  and obtained  $C = 7.6$ , where  $\sigma$  is the surface tension coefficient. In similar experiments performed in Ref. [36], values for  $C$  ranging from 5.45 in oil-wet porous media to 306.25 in water-wet porous media were obtained. The curvature in Eq. (9) can be rewritten in spherical coordinates as [39]

$$\left[ \frac{1}{r_a} + \frac{1}{r_b} \right] = \frac{2}{R} - \frac{2\zeta + \nabla_{\omega}^2 \zeta}{R^2} + O(\zeta^2), \quad (10)$$

where  $\nabla_{\omega}^2$  is the Laplace operator on the unit sphere,

$$\nabla_{\omega}^2 = \frac{1}{\sin \theta} \frac{\partial}{\partial \theta} \left( \sin \theta \frac{\partial}{\partial \theta} \right) + \frac{1}{\sin^2 \theta} \frac{\partial^2}{\partial \phi^2}. \quad (11)$$

In the following calculation, we use the spherical harmonics property

$$\nabla_{\omega}^2 Y_{lm} = -l(l+1) Y_{lm}. \quad (12)$$

To obtain the equation of motion for the perturbation amplitudes  $\zeta_{lm}$ , first we substitute Eq. (10) into the pressure jump condition (9). Then, we place the result of this procedure plus Eq. (7) into Eq. (6). Always keeping terms up to first order in  $\zeta$ , and using the orthonormality of the spherical harmonics, we find the *dimensionless* equation of motion for the perturbation amplitudes,

$$\dot{\zeta}_{lm}(t) = \lambda(l, R, \dot{R}) \zeta_{lm}(t), \quad (13)$$

where

$$\lambda(l, R, \dot{R}) = \frac{\dot{R}}{R} (l-1) - \frac{1}{\text{Ca} R^3} (l+2)(l^2-1) \quad (14)$$

is the linear growth rate. In Eq. (13), length and time are rescaled by characteristics length  $L$  and time  $T$ , respectively. Moreover,

$$\text{Ca} = \frac{\eta U L^2}{\sigma^* k} \quad (15)$$

represents a modified capillary number with  $U = L/T$  [31]. The solution of Eq. (13) is given by

$$\zeta_{lm}(t) = \zeta_{lm}(0) \exp\{I(l, R, \dot{R})\}, \quad (16)$$

where

$$I(l, R, \dot{R}) = \int_{t_c(l)}^t \lambda(l, R, \dot{R}) dt', \quad (17)$$

with  $t_c(l)$  being the time at which a mode  $l$  becomes unstable [ $\lambda(l) = 0$ ]. Here, it is assumed that  $\zeta_{lm}(t) = \zeta_{lm}(0)$  if  $0 \leq t < t_c(l)$  [8].

Important linear information can be obtained by Eq. (14). The mode of maximum growth rate is calculated by setting  $d\lambda(l, R, \dot{R})/dl = 0$ , yielding

$$l_{\max}(R, \dot{R}) = \sqrt{\frac{7}{9} \left(1 + \frac{3}{7} \text{Ca} \dot{R} R^2\right) - \frac{2}{3}} \approx \sqrt{\frac{1}{3} \text{Ca} \dot{R} R^2}. \quad (18)$$

In Eq. (18) we used  $\text{Ca} \dot{R} R^2 \gg 1$  since for typical porous media experiments  $\text{Ca} \dot{R} R^2$  is very large [28].

### B. Variational approach for the optimal injection rate

In this section, our goal is to minimize the perturbations amplitudes (16). This can be performed by extremizing the integral (17). Keeping in mind that  $l_{\max}$  is the fastest growing mode, we focus on minimizing the integral

$$I(l_{\max}, R, \dot{R}) = \int_0^t \lambda(l_{\max}, R, \dot{R}) dt', \quad (19)$$

where  $t_c(l_{\max}) = 0$ , and using  $\text{Ca} \dot{R} R^2 \gg 1$  we have

$$\lambda(l_{\max}, R, \dot{R}) \approx \frac{2}{3} \sqrt{\frac{\text{Ca}}{3}} \dot{R}^{3/2} - \frac{5\dot{R}}{3R}, \quad (20)$$

which only depends on  $R$  and  $\dot{R}$ . Recall that we want to inject a certain amount of the inviscid fluid by keeping fixed initial and final radii during a time interval  $[0, t_f]$ . In this way,  $I$  in Eq. (19) is the *action*, while  $\lambda$  defines the *Lagrangian* of the system. Thus, we actually have a variational problem which can be solved by using the Euler-Lagrange equation,

$$\frac{d}{dt} \left( \frac{\partial \lambda}{\partial \dot{R}} \right) = \frac{\partial \lambda}{\partial R}, \quad (21)$$

with fixed end points  $R(t=0) = R_0$  and  $R(t=t_f) = R_f$ . From now on, we take  $L$  as being the dimensional final radius and  $T$  as the dimensional final time of the injection process. By doing this, we have  $R_f = 1$  and  $t_f = 1$ . Substitution of the growth rate (20) into Eq. (21) leads to a very simple differential equation  $\ddot{R} = 0$ , whose solution is

$$R(t) = R_0 + (1 - R_0)t. \quad (22)$$

From Eq. (3),  $Q(t) = 4\pi \dot{R} R^2$ , and the optimal pumping rate is given by

$$Q(t) = 4\pi(1 - R_0)[R_0 + (1 - R_0)t]^2. \quad (23)$$

We conclude that the injection rate must vary quadratically with time in order to minimize the perturbation amplitudes. Note that the optimal solution is not any quadratic function, but precisely the one prescribed by Eq. (23). Furthermore, it

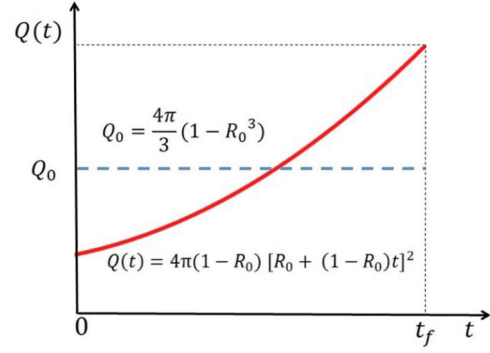


FIG. 1. (Color online) Sketch of the injection rate as a function of time for the optimal injection  $Q(t)$  (solid line) and the equivalent constant injection rate  $Q_0$  (dashed line). The total volume of injected fluid (area under the curves) in the interval  $[0, t_f]$  should be the same for both pumping rates.

is interesting to note that our optimal pumping rate (23) does not depend either on the material properties of the fluids or on the properties of the medium.

### III. THEORETICAL DISCUSSION

In this section, we study theoretically the efficacy of the variational protocol based on the optimal injection rate (23). Usual radial viscous-fingering flow considers insertion of a specific volume of fluid at a constant injection rate. Under such a circumstance, the dimensionless version of Eq. (3) with  $R_f = 1$  and  $t_f = 1$  is

$$Q_0 = \frac{4\pi}{3} (1 - R_0^3). \quad (24)$$

Now, our task is to compare the resulting interface morphology obtained by using the constant injection rate (24) and the ideal pumping rate (23) at  $t = t_f$ . An illustrative representation of the behavior of  $Q(t)$  and  $Q_0$  as time progresses is given in Fig. 1. We begin our analysis by inspecting Fig. 2.

The results presented in Fig. 2 are obtained by setting  $R_0 = 0.2$  and  $\text{Ca} = 650$ . The value of the modified capillary

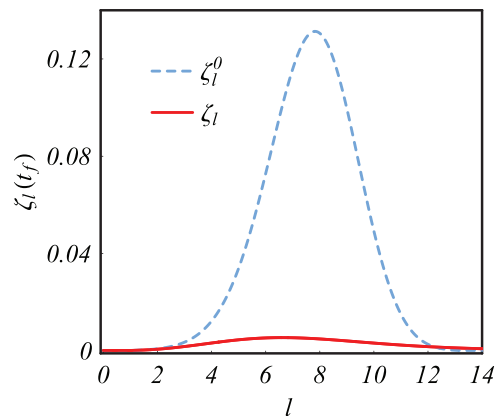


FIG. 2. (Color online) Plot of the amplitude Eq. (2) as a function of mode  $l$  at  $t = t_f$ . The solid curve represents the amplitude for the optimal injection rate (23), and the dashed curve represents the amplitude for the constant injection process (24).

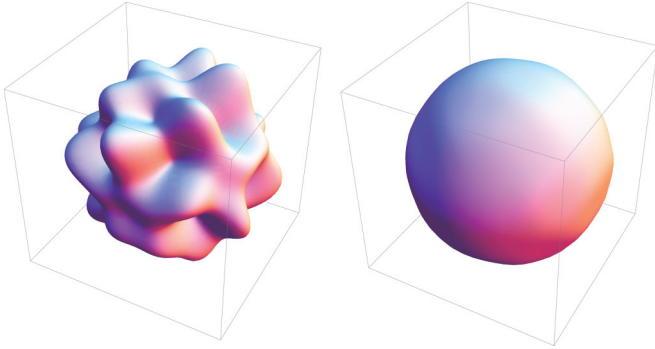


FIG. 3. (Color online) Resulting interfacial patterns at  $t = t_f$  by utilizing the constant injection (left panel) and optimal injection (right panel).

number  $Ca$  is consistent with the physical parameters used in typical experimental realizations of porous media flows [28]. Figure 2 plots the amplitude given by Eq. (2) at  $t_f$  for the optimal pumping  $\zeta_l(t_f)$  (solid curve) and for the equivalent constant flux injection  $\zeta_l^0(t_f)$  (dashed curve) as functions of the wave number  $l$ . Here we adopted the notation  $\zeta_{lm} = \zeta_l$ . By examining this figure, we can readily see a substantial reduction of the final perturbation amplitudes when the ideal injection is used. The physical explanation for the success of the optimum stabilization method [Eq. (23)] is based on the fact that initially  $Q(t)$  is sufficiently small, so that the front evolves with a sizable unperturbed shape. As time progresses, the pumping increases appreciably, but as long as it takes place at a large interfacial radius, the injection is no longer able to promote a considerable destabilization of the propagating front. In other words, the onset of instability is delayed, and when it eventually occurs, disturbances arise with a reduced growth rate.

In Fig. 3, we can clearly see the efficiency of the optimal injection process. The left panel of Fig. 3 plots the resulting interface for the constant injection rate, and the right panel of Fig. 3 illustrates the resulting interface for the ideal pumping situation. Here we set  $R_0 = 0.2$  and  $Ca = 650$ . The patterns have the same initial conditions (including the random phases attributed to each mode), and 18 modes have been considered. It is evident that finger formation is considerably inhibited on the interface shown in the right panel of Fig. 3.

It is important to analyze the robustness of our ideal injection process when  $Ca$  is increased. Regarding this point, Fig. 4 plots the maximum amplitude for the constant pumping situation divided by the maximum amplitude calculated by using the optimal injection rate [ $\zeta^0(t_f)/\zeta(t_f)$ ] as a function of  $Ca$ , at final time  $t = t_f$ . We consider two values of  $R_0$ . From this figure it is clear that the ratio  $\zeta^0(t_f)/\zeta(t_f)$  grows when  $Ca$  is increased, and when smaller values of  $R_0$  are considered. Of course, since  $t_f$  and  $R_f$  can be large, the final optimal injection interface can indeed present some undulations. However, Fig. 4 shows that the amplitudes of such perturbations are guaranteed to be considerably smaller than the ones obtained by the equivalent constant pumping process, even when a higher constant injection rate (larger  $Ca$  and a lower value of  $R_0$ ) is considered. Moreover, this behavior also indicates that the stabilization of the variational approach still remains if we

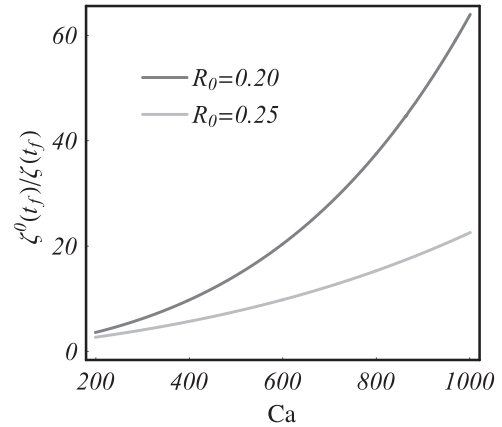


FIG. 4. Amplitude ratio  $\zeta^0(t_f)/\zeta(t_f)$  as a function of  $Ca$ , for  $R_0 = 0.2, 0.25$ . Here  $\zeta^0(t_f)$  [ $\zeta(t_f)$ ] denotes the maximum amplitude for constant (optimal) injection at  $t = t_f$ .

want a longer evolution of the interface. It is worthwhile to mention that the capillary number cannot be arbitrarily large, otherwise wetting and other complex effects would have to be considered in the theory.

#### IV. CONCLUSION

The possibility of inhibiting viscous fingering in porous media is of great importance to science and technology, mainly to oil extraction industries. During oil recovery by water from petroleum reservoirs, preferential channeling of water flow is caused in part by viscous driven instability. This results in a significant reduction in oil extraction from the porous medium. Keeping this fact in mind, we deduced a linear growth rate of a radially growing interface that separates two immiscible fluids, with different viscosities, in a three-dimensional uniform porous medium. We used an analytical variational approach to look for the optimal injection rate in order to minimize the perturbations amplitude at the interface. By using this method, we found that disturbances are restrained if the injection rate evolves with time in a specific quadratic function. To verify the suitability of the minimization method at a linear level, we observed that the stabilization protocol is robust even when a larger capillary number is considered.

A natural extension of this work would be the investigation of fully nonlinear stages of the dynamics through computer simulations and experiments. Moreover, the application of the variational protocol to a more complete theoretical model for porous media flow would be interesting: considering fluids with distinct densities, variations in the saturations behind the front, heterogeneity of the medium, and capillary pressure drop across the interface depending on the velocity of the front. This variational approach and possible generations can provide a step forward toward ultimate control of porous media viscous fingering.

#### ACKNOWLEDGMENTS

I thank CNPq for financial support, and I am very grateful to José Miranda for a critical reading of this work.

- [1] P. G. Saffman and G. I. Taylor, *Proc. R. Soc. London, Ser. A* **245**, 312 (1958).
- [2] For review papers, see K. V. McCloud and J. V. Maher, *Phys. Rep.* **260**, 139 (1995); J. Casademunt, *Chaos* **14**, 809 (2004).
- [3] S. B. Gorell and G. M. Homsy, *SIAM J. Appl. Math.* **43**, 79 (1983).
- [4] B. Jha, L. Cueto-Felgueroso, and R. Juanes, *Phys. Rev. Lett.* **106**, 194502 (2011).
- [5] X. Cheng, L. Lu, A. Patterson, H. M. Jaeger, and S. R. Nagle, *Nat. Phys.* **4**, 234 (2008).
- [6] H.-Y. Chu and H.-K. Lee, *Phys. Rev. Lett.* **107**, 225001 (2011).
- [7] A. C. Callan-Jones, J.-F. Joanny, and J. Prost, *Phys. Rev. Lett.* **100**, 258106 (2008).
- [8] E. O. Dias, E. Alvarez-Lacalle, M. S. Carvalho, and J. A. Miranda, *Phys. Rev. Lett.* **109**, 144502 (2012).
- [9] A. He, J. S. Lowengrub, and A. Belmonte, *SIAM J. Appl. Math.* **72**, 842 (2012).
- [10] L. dos Reis and J. A. Miranda, *Phys. Rev. E* **84**, 066313 (2011).
- [11] C.-Y. Chen, C.-W. Huang, L.-C. Wang, and J. A. Miranda, *Phys. Rev. E* **82**, 056308 (2010).
- [12] E. O. Dias, F. Parisio, and J. A. Miranda, *Phys. Rev. E* **82**, 067301 (2010).
- [13] E. O. Dias and J. A. Miranda, *Phys. Rev. E* **81**, 016312 (2010).
- [14] A. Leshchiner, M. Thrasher, M. B. Mineev-Weinstein, and H. L. Swinney, *Phys. Rev. E* **81**, 016206 (2010).
- [15] S. W. Li, J. S. Lowengrub, J. Fontana, and P. Palffy-Muhoray, *Phys. Rev. Lett.* **102**, 174501 (2009).
- [16] T. T. Al-Housseiny, P. A. Tsai, and H. A. Stone, *Nat. Phys.* **8**, 747 (2012).
- [17] D. Pihler-Puzović, P. Illien, M. Heil, and A. Juel, *Phys. Rev. Lett.* **108**, 074502 (2012).
- [18] F. M. Rocha and J. A. Miranda, *Phys. Rev. E* **87**, 013017 (2013).
- [19] F. M. Rocha and J. A. Miranda, *Phys. Rev. E* **88**, 033008 (2013).
- [20] N. Mungan, *Can. J. Chem. Eng.* **49**, 32 (1971).
- [21] H. J. Pearson, *The Stability of Some Variables Viscosity Flow with Application in Oil Extraction* (Cambridge University Press, Cambridge, 1977).
- [22] D. Shar and R. Schechter, *Improved Oil Recovery by Surfactants and Polymer Flooding* (Academic, New York, 1977).
- [23] R. L. Slobod and J. S. Lestz, *Prod. Monthly* **24**, 12 (1960).
- [24] F. Fayers, *Enhanced Oil Recovery* (Elsevier, Amsterdam, 1981).
- [25] G. Pope, *Soc. Petrol. Eng. J.* **20**, 191 (1980).
- [26] P. Daripa and G. Pasa, *Int. J. Eng. Sci.* **42**, 2029 (2004).
- [27] P. Daripa and X. Ding, *Transp. Porous Med.* **93**, 675 (2012).
- [28] R. L. Chuoke, P. van Meurs, and C. van der Poel, *Petrol. Trans. AIME* **216**, 188 (1959).
- [29] S. P. Neuman and G. Chen, *Water Resour. Res.* **32**, 1891 (1996).
- [30] J. P. Stokes, D. A. Weitz, J. P. Gollub, A. Dougherty, M. O. Robbins, P. M. Chaikin, and H. M. Lindsay, *Phys. Rev. Lett.* **57**, 1718 (1986).
- [31] G. M. Homsy, *Annu. Rev. Fluid Mech.* **19**, 271 (1987).
- [32] G. Chen and S. P. Neuman, *Phys. Fluids* **8**, 353 (1996).
- [33] A. Tartakovsky, S. P. Neuman, and R. J. Lenhard, *Phys. Fluids* **15**, 11 (2003).
- [34] I. White, P. M. Colombera, and J. R. Philip, *Soil Sci. Soc. Am. J.* **41**, 483 (1976).
- [35] H. J. de Haan, *Proceedings of the 5th World Petroleum Congress* (World Petroleum Congress, New York, 1959), Sec. II, p. 544.
- [36] E. J. Peters and D. L. Flock, *Soc. Pet. Eng. J.* **21**, 249 (1981).
- [37] L. Paterson, V. Hornof, and G. Neale, *Rev. Inst. Fr. Pet.* **39**, 517 (1984).
- [38] G. B. Arfken, H. J. Weber, and F. E. Harris, *Mathematical Methods for Physicists: A Comprehensive Guide* (Academic, New York, 2013).
- [39] M. Fontelos and A. Friedman, *Arch. Ration. Mech. Anal.* **172**, 267 (2004).